



**Michigan
Technological
University**

Michigan Technological University
Digital Commons @ Michigan Tech

Dissertations, Master's Theses and Master's Reports

2019

CRACK PATTERN SIMULATION OF PRESSURIZED BOROSILICATE GLASS TUBE UNDER PELLET IMPACT USING ALE METHOD

Omkar Bhumkar

Copyright 2019 Omkar Bhumkar

Follow this and additional works at: <https://digitalcommons.mtu.edu/etdr>



Part of the [Computer-Aided Engineering and Design Commons](#)

CRACK PATTERN SIMULATION OF PRESSURIZED BOROSILICATE GLASS
TUBE UNDER PELLET IMPACT USING ALE METHOD

By

Omkar S. Bhumkar

A REPORT

Submitted in partial fulfillment of the requirements for the degree of

MASTER OF SCIENCE

In Mechanical Engineering

MICHIGAN TECHNOLOGICAL UNIVERSITY

2019

© 2019 Omkar S. Bhumkar

This report has been approved in partial fulfillment of the requirements for the Degree of MASTER OF SCIENCE in Mechanical Engineering.

Department of Mechanical Engineering – Engineering Mechanics

Report Advisor: *Dr. Gregory Odegard*
Committee Member: *Dr. Stephen Morse*
Committee Member: *Dr. Trisha Sain*

Department Chair: *Dr. William Predebon*

Table of Contents

List of figures.....	v
List of tables.....	vi
Abstract.....	vii
1 Introduction.....	1
1.1 Scope.....	2
1.2 Previous Work.....	2
1.2.1 Pellet and Glass Tube Modelling.....	3
1.2.2 Glass Failure Model.....	5
1.3 Experimental Set-up.....	5
2 Finite Element Model Setup.....	8
2.1 Arbitrary Lagrangian Eulerian Technique.....	8
2.2 Boundary Conditions.....	9
2.3 Meshing:.....	9
2.4 Equation of State.....	10
2.5 Contact modelling.....	12
2.5.1 Pressurized Fluid Motion.....	12
2.5.2 Coupling/ Interaction between Pressurized air and Glass tube.....	12
2.6 Failure strain calculation.....	14
3 Challenges and Limitations.....	18
3.1 *Constrained_Lagrange_in_Solid contact parameter calibration.....	18
3.2 Meshing.....	18
3.3 Size of output files.....	19
3.4 Internal Pressures.....	19
4 Results and Correlation.....	20
4.1 Comparison of Results for 3.5e-5 and 4.45e-4 Failure Strain.....	20
4.2 Verification of Results.....	21
4.3 Correlation with Experimental Data.....	21

5 Conclusion24

6 Recommendations.....25

7 Reference List26

A Appendix.....27

 A.1 Properties of Borosilicate Glass27

 A.2 LS-Dyna Card Images28

 A.2.1 Equation of state card image.....28

 A.2.2 ALE Reference System Group card image28

 A.2.3 Constrained Lagrange in Solid Contact card image29

List of figures

Figure 1. Bushing mounted on oil filled transformer [1].....	1
Figure 2. Pellet and glass tube modelling	3
Figure 3. Recommended glass tube gradient mesh.....	4
Figure 4. Experimental setup – pressurized glass tube mounted on a fixture.....	5
Figure 5. 0.22 caliber pellet used for impact in experiment	6
Figure 6. Images captured by high speed camera during crack propagation.....	6
Figure 7. Simulation setup	9
Figure 8. Mesh pattern and size	10
Figure 9. Standard penalty-based coupling.....	13
Figure 10. Required shell normal for fluid detection by code	14
Figure 11. Stress applied to infinite plate with elliptical hole	15
Figure 12. Assumption of elliptical flaw as crack	16
Figure 13. Load curve defining d3plot output interval	19
Figure 14. Glass tube shattering at $t= 0.01$ ms for $3.5e-5$ failure strain	20
Figure 15. Average pressure Vs time output from dbfsi file	21
Figure 166. Stills from pellet impact experiment for 50, 65 and 100 psi internal pressure	22
Figure 17. Crack pattern after pellet impact for 50, 65 and 100 psi internal pressure.....	22

List of tables

Table 1. Specifications of 0.22 caliber pellet.....	3
Table 2. Specifications of glass tube.....	3
Table 3. Material properties of pellet.....	4
Table 4. Material properties of glass tube.....	4
Table 5. Experimental test results.....	7
Table 6. Type of elements used in simulation	9
Table 7. Comparison of broken glass size between simulation and experiment	23

Abstract

Transformer bushings are a common target for sniper attacks to cause power failure in large areas. Given the size, internal pressure and brittle nature of transformer bushing, pellet impact causes damage to surrounding components due to broken bushing pieces. To mitigate this, a project was initiated by United States Bureau of Reclamation to develop a safety mechanism. Finite Element Analysis is proposed to optimize and reduce cost of the design.

A simplified Finite Element model is created which consists of 0.22 caliber lead pellet impacting Pyrex 7740 borosilicate glass tube. Previous studies on the effect of the mesh pattern, size and cap geometry were carried out. One of the biggest factors which can help in mitigating the transformer component damage is internal pressure of bushing fluid. This study focuses on developing a Finite Element model which captures the fluid-structure interaction between glass tube and internal pressurized air. Arbitrary Lagrangian Eulerian code of LS-DYNA is used to simulate this interaction.

This report describes the modelling techniques used to simulate the pellet impact on pressurized tube. Failure strain calculations are also discussed in the report. The effect of internal pressure and failure strain are addressed. Crack pattern and broken glass fragments size are considered for a comparison between the pellet impact simulation and experiment.

1 Introduction

Today, electricity has become an irreplaceable part of human lives. This electricity is produced at different kinds of power plants including Hydroelectric, Nuclear, Thermal, Wind, Solar. These power plants are situated away from the high population areas. This is where the power grid comes into picture which transfers electricity generated at power plant to various consumer locations.

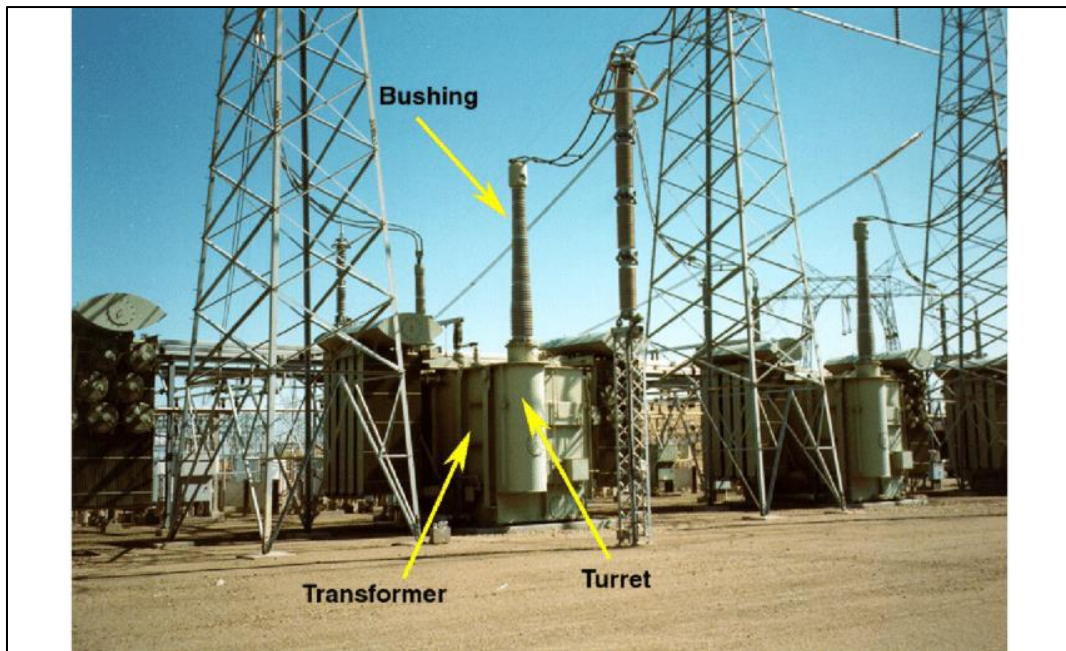


Figure 1. Bushing mounted on oil filled transformer [1]

Transformers are key part of power grid where they boost the voltage from power plants for transmission of electricity to hundreds of miles and then reduce the voltage to under 10,000 V when the electricity reaches substations. [2] Failure of these transformers can lead to complete blackout to major part of population and can cost millions of dollars along with months of repairs to get the power grid back up.

Such failure occurred on April 16th, 2013 at Cayote, California, due to attack on substation where a shooter shot 17 transformers and 6 circuit breakers causing 15.4 million dollars in damage.[3] Bushings are used for protecting and guiding high voltage power lines. They are mounted on top of the transformers and visible from long distance making them a attractive target for such shooters.

United States Bureau of Reclamation oversees the water and hydroelectric power supply in 17 western states. They have planned to build a safety mechanism to protect transformers from events like shootings in California. Bushings are made of insulating material like porcelain and have borosilicate sight glass on top. These bushings can be filled with oil or air for cooling purpose. Under pellet impact, shattered porcelain or glass pieces can result

in failure of surrounding structures. Modifying the design of bushings can be effective to avoid transformer failures under ballistic impact.

The goal of this project is to modify bushing design reduce large pieces of porcelain/glass which can harm its surrounding transformer components. This can be achieved by using material like laminated glass or by fragmentizing porcelain/glass into small particles by manipulating inside air/oil pressure under pellet impact. Due to numerous combinations of design modifications, finding a material or internal pressure using lab testing will lead to huge cost. To minimize the cost, only few experimental tests were done using simple glass tubes under various internal pressures. These are used to calibrate a Finite Element model which can be further used to find most cost-effective design by changing the design parameters such as geometry, material or inside pressure.

1.1 Scope

In this study, a finite element model of pressurized glass tube is created to simulate the ballistic impact on transformer bushings. This study will explore the effect of internal pressure on fragmentation of glass tube using Arbitrary Lagrangian Eulerian (ALE) method. The FE model is built upon the work and suggestions by previous students who worked on this project. [4,5]

Research has been conducted to implement ALE method in FE model to simulate interaction between the internal pressurized fluid and glass tube. To simplify the model, internal fluid is assumed as an ideal gas in the simulation. The end goal of this study to capture the fluid-structure interaction during the impact event to match experimental results. Calibration of the FE model is done based on two parameters: 1. Crack Pattern 2. Broken Glass Size.

1.2 Previous Work

Sandesh Gandhi [4] has laid the groundwork for the project. LS-Dyna solver has been used for simulation. He studied the effect of mesh pattern, size and the failure strain in detail with constant internal pressure (10 psi). He concluded the oval mesh pattern with a mesh size of 0.25 mm matches better with experimental results. Also, a $3.5e-5$ failure strain was recommended after comparison with crack pattern found in experiments.

Taking the FE model further, Vijay Thanati [5] worked on gradient mesh sizes to reduce the computational cost of simulation. Additionally, he studied the effect of glass tube cap geometry and internal pressure on fragmentation of glass tube. By comparing results, an estimated curve was selected to take pressure drop after impact in account. Broken glass size was compared for calibration of FE model.

Details of previous FE models are discussed in next sections.

1.2.1 Pellet and Glass Tube Modelling

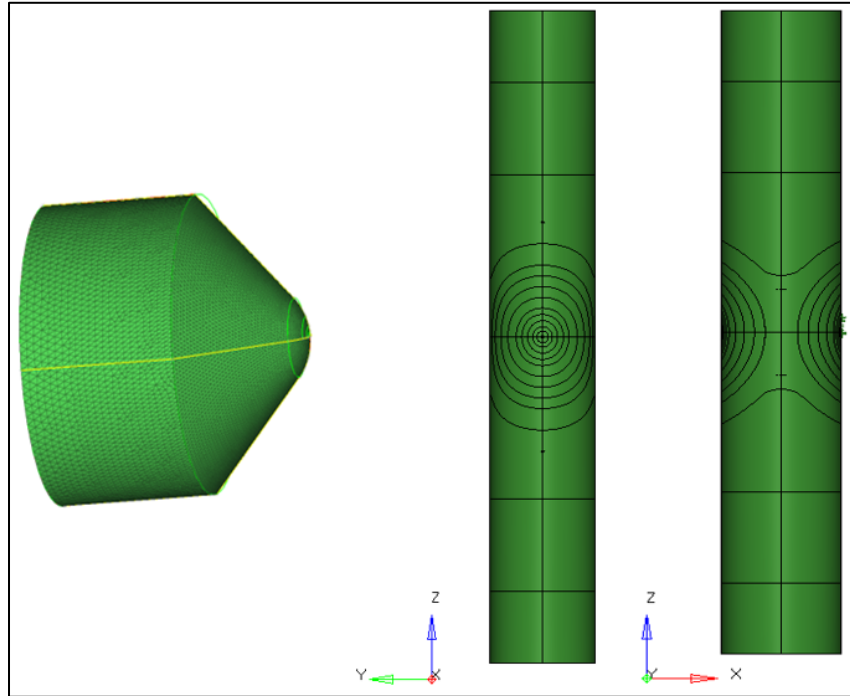


Figure 2. Pellet and glass tube modelling

A simple FE model was created by Sandesh Gandhi [4] to simulate ballistic impact on glass tube. Figure 2 shows the enhanced image of projectile and the glass tube with oval pattern. Several mesh patterns were explored, and it was found the oval mesh pattern simulates better crack pattern closest to experiments. Table 1 and 2 shows the specifications of 0.22 caliber lead pellet and glass tube.

Table 1. Specifications of 0.22 caliber pellet

Diameter	5.5 mm
Mass	0.93 grams
Estimated slope of the tip	45 degrees
Cylindrical part height	3.37 mm
Material	Cast Lead

Table 2. Specifications of glass tube

Height	12 inches = 304.8 mm
Thickness	0.25 inch = 6.35 mm
Diameter	2 inch = 50.8 mm
Material	Pyrex 7740 borosilicate glass

The pellet is meshed with tetrahedral elements of 0.05 mm to 0.15 mm size. The glass tube is meshed with 1st order fully integrated (Element formulation= 16) shell elements including quad and tria elements. Vijay Thanati [5] studied the effect of mesh size and concluded that the mesh size of minimum length of 0.1 at the center and then gradient mesh of 0.4 mm to 1.6 mm at either side of glass tube is computationally economical and matches well with experimental data. Figure 3 shows the recommended gradient mesh for glass tube.

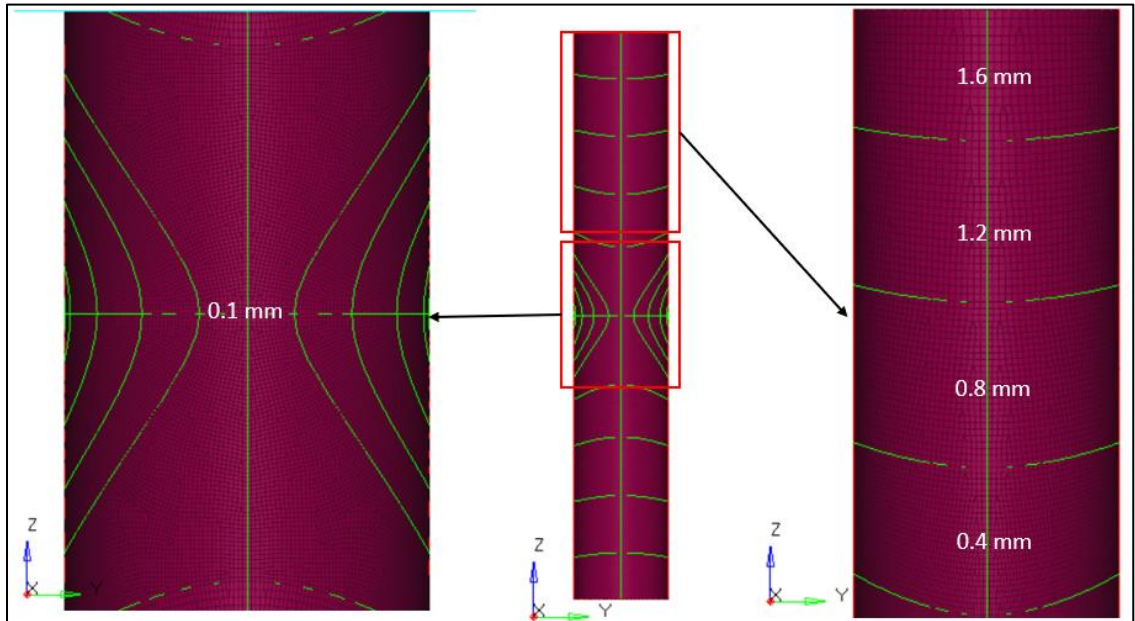


Figure 3. Recommended glass tube gradient mesh

To account for strain hardening and future scope for including strain rate effects in future *MAT_PLASTIC_KINEMATIC is used. For glass tube, *MAT_LAMINATED_GLASS along with *MAT_ADD_EROSION is used. *MAT_LAMINATED_GLASS is usually used for layered glasses which have polymer layers. In material card, polymer layer definition is turned off to simulate the borosilicate glass used in experiments. In future, polymer layer definition can be turned on to find effect of laminated glass on bushing failures. Table 3 and 4 shows the material properties of pellet and glass tube. See Appendix A.1 for manufacturer's specifications of glass tube material.

Table 3. Material properties of pellet

Density	11.34 g/cc
Young's modulus	14 GPa
Poisson's Ratio	0.42
Yield Stress	0.250 GPa
Tangent Modulus	0.9

Table 4. Material properties of glass tube

Composition	81%, Na ₂ O: 4%, K ₂ O: 0.5%, B ₂ O ₃ : 13%, Al ₂ O ₃ : 2%
Density	2.23 g/cc
Young's modulus	63 GPa
Poisson's Ratio	0.20
Shear Modulus	26.1 GPa
Yield Stress	70 MPa (assumed)

1.2.2 Glass Failure Model

*MAT_ADD_EROSION is used to simulate the crack pattern in glass tube after pellet impact. Maximum principal strain is used as a failure criterion i.e. when an element will reach specified maximum principal strain, that element will be deleted from the analysis. After studying the effect of failure strain on crack pattern, Sandesh Gandhi concluded that the results comparison is better with 3.5e-5 failure strain.

1.3 Experimental Set-up

The United States Bureau of Reclamation conducted an experiment of ballistic impact with 0.22 caliber pellet on borosilicate glass tube to study the crack propagation event. The simple borosilicate glass tube was chosen instead of an actual bushing to reduce the complexity and cost of experiment assuming the effect of geometric changes is negligible in crack propagation/pattern. Figure 4 shows the experimental test setup. In Figure 4, enclosed glass tube is mounted at the bottom with a fixture to restrict its degrees of freedom in all directions. An internal pressure on glass tube can be applied with a fixture to study the effect of various pressure on fragmentation of glass under pellet impact. Experiment is done for pressures ranging from 0 to 100 psi. A high-speed camera is mounted from side to capture the crack pattern during the impact event.

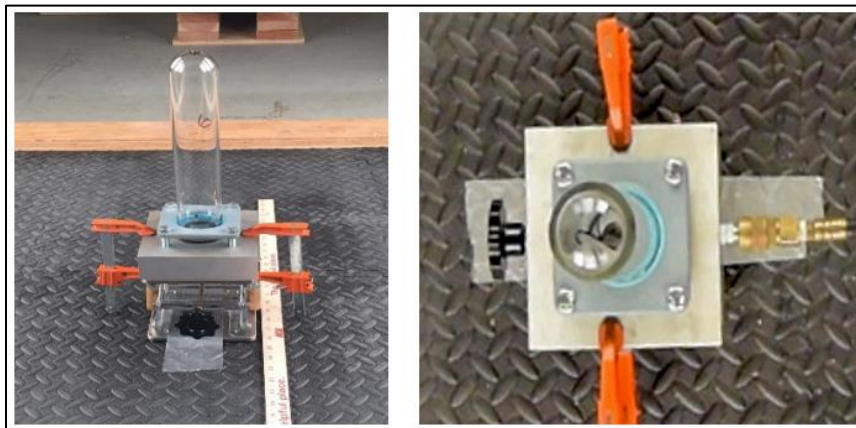


Figure 4. Experimental setup – pressurized glass tube mounted on a fixture

A 0.22 caliber pellet shown in Figure 5 is fired into glass tube with the velocity of 1100 fps which is approximately 335.280 m/s. For each internal pressure, images were captured throughout the impact event starting from the time pellet hits the tube till it leaves from the other end. Figure 6 shows the images captured during impact event with pellet entering from the right for 0 psi and 10 psi.



Figure 5. 0.22 caliber pellet used for impact in experiment

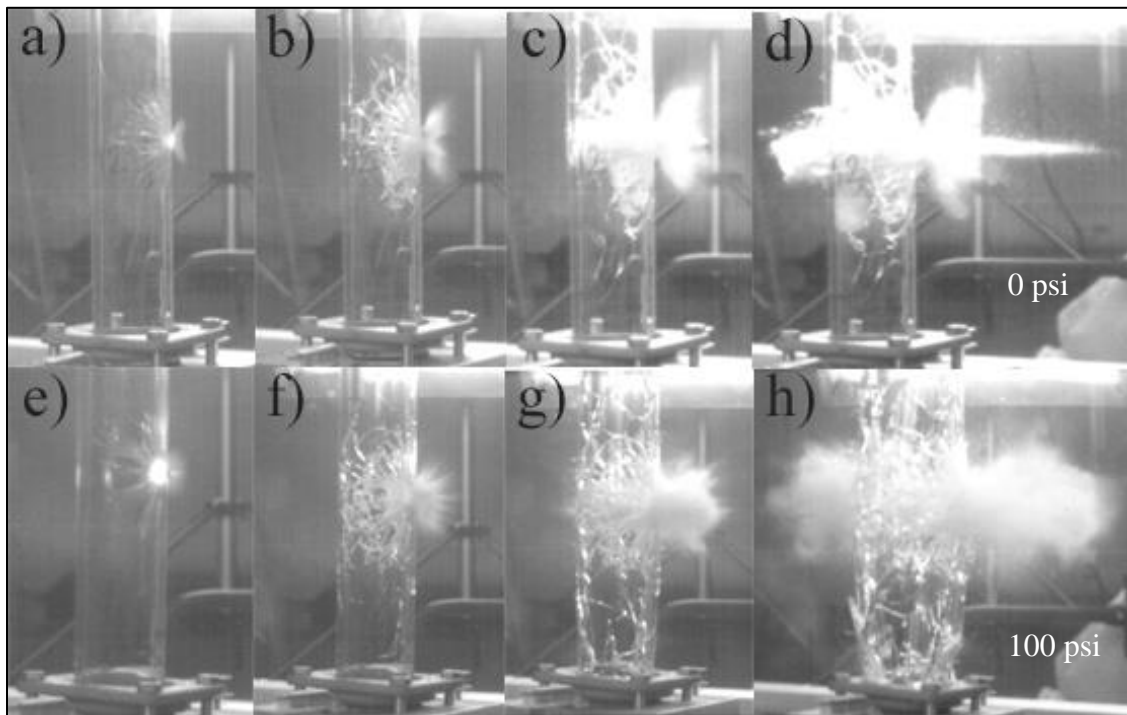


Figure 6. Images captured by high speed camera during crack propagation

Along with image capturing, USBR also collected 10 largest broken glass pieces for different internal pressures. Table 5 shows the approximate maximum and average surface area of found pieces for 0-100 psi internal pressures.

Table 5. Experimental test results

Sr. No.	Internal Pressure (psi)	Average Surface Area (cm²)	Maximum Surface Area (cm²)
1	0	18.303	55.892
2	10	16.089	41.762
3	30	13.766	26.900
4	50	14.009	24.734
5	65	9.167	18.280
6	75	10.014	14.960
7	100	7.751	15.959

From the captured images and broken glass samples following observations were made:

1. Crack pattern: Crack propagation pattern is in radial direction in the vicinity of impact. It changes to vertical or horizontal direction as we go farther away from impact location.
2. Glass size: At impact location where pellet enters and leaves the glass tube, glass pulverizes instantly. As we go farther away from impact location, broken glass size increases.
3. Effect of internal pressure: From images and the surface areas calculated, it's clear that as internal pressure increase, the size of broken glass decreases.

2 Finite Element Model Setup

Finite element model used in this project is built on the recommendations and conclusions of previous work. In previous studies, to simulate the internal pressure on glass tube, nodal pressure was used. The pressure was kept either constant or was estimated after the pellet impact. The drawback of this method was the pressure drop after pellet impact was not captured accurately. This study utilizes ALE finite element code developed by LS-Dyna to simulate the fluid structure interaction between pressurized internal air and glass tube. Type of elements, mesh pattern and size were modified to make the finite model compatible with the ALE method. Hypermesh v14.0 to set-up finite element model and Kg, mm, ms unit system is used for the same.

Important details of simulation setup have been explained further in this section.

2.1 Arbitrary Lagrangian Eulerian Technique

An important factor in developing the counter measure of bushing failure is the effect of internal pressure. To get accurate results, it is vital to capture the pressure drop after the pellet impact. Pellet impact involves the sudden flow of pressurized air after glass tube is broken. The material motion can be defined using two methods in fluid or structural dynamics: Lagrangian and Eulerian

In the Lagrangian method, mesh or nodes are fixed in space; when material deforms, nodes deform with material. If a Lagrangian mesh is used to simulate a fluid, elements will go through large deformations which introduces numerical inaccuracies in results. Also, these large deformations can result in extremely small time step which increases computational time exponential and can lead to numerical instability during analysis. Due to these reasons, the Lagrangian method is usually used in structural analysis than fluid flow.

In Eulerian method, mesh or nodes are fixed in space but material can flow freely within mesh. The Eulerian method uses Navier-Stokes equations for analysis which are computationally expensive and more complicated than lagrangian method.

To take an advantage of these two methods, a hybrid numerical algorithm was developed called Arbitrary Lagrangian Eulerian. Arbitrary Lagrangian Eulerian algorithm involves material deformation as in Lagrangian method and remapping/ advection of Lagrangian elements back to moving Eulerian mesh i.e. in this method, mesh or nodes can move arbitrarily in space and material will flow freely through the moving mesh. This allows large mesh deformation while keeping the quality of mesh intact.

Suitable material models and equation of states are available in ALE for modelling pressurized fluid. Furthermore, coupling and advection algorithms are provided in this finite element code to calculate accurate results. Pressure of each element is calculated at every time step based on the equation of state defined for model.

2.2 Boundary Conditions

Figure 7 shows Finite Element Model which best models the experimental test setup with glass tube with pressurized air inside. The enclosing fixed plate at the bottom is modelled as a rigid body which represents to mounting of the tube in experiment. *MAT_RIGID material is assigned to fixed plate component and all degrees of freedom are constrained. Initial velocity of 1100 fps (approximately 335.280 m/s) is applied to pellet using *INITIAL_VELOCITY_GENERATION. To ensure that the pellet doesn't hit the glass tube until the specified pressure is applied on glass, initial velocity is applied 0.5 ms after the start of simulation. This time is decided after few trial simulations and is implemented using *INITIAL_VELOCITY_GENERATION_START_TIME.

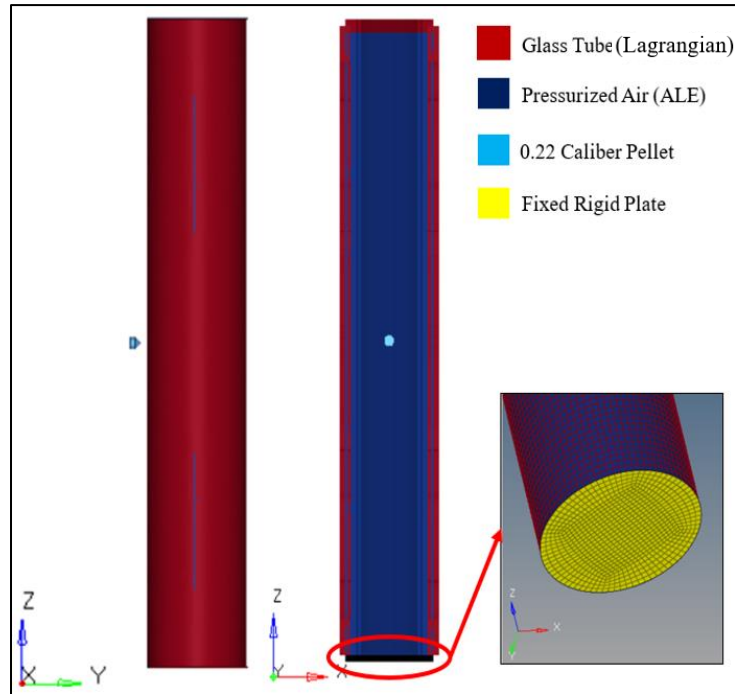


Figure 7. Simulation setup

2.3 Meshing:

Table 6 shows the type of elements used for all components of setup.

Table 6. Type of elements used in simulation

Sr. No.	Component	Element Type	Element Formulation
1	Glass Tube	Shell	ELFORM = 16
2	Pressurized Air	Hexahedral	ELFORM = 11
3	Pellet	Tetrahedral	ELFORM = 1
4	Bottom Fixed Plate	Shell	ELFORM = 16

Initially, glass tube was meshed as per the recommendation of Vijay Thanati [5] with oval mesh pattern at both sides of glass tube with x4 variant gradient mesh. At point of impact, 0.1 mm size mesh is used and 0.4 mm to 1.6 mm variation is used as we go farther away from impact origin. Hexahedral mesh for pressurized air component is created with similar gradient mesh as glass tube. Computational cost required for recommended x4 gradient mesh was around 200-250 hours.

To reduce the computational cost, number of iterations were carried out for different gradient mesh size. Trade-off between quality of results and mesh size was found for a gradient mesh varying from 0.2 mm at impact position to 1.6 mm farther away from center of impact was selected. Figure 8 shows the selected mesh pattern and size.

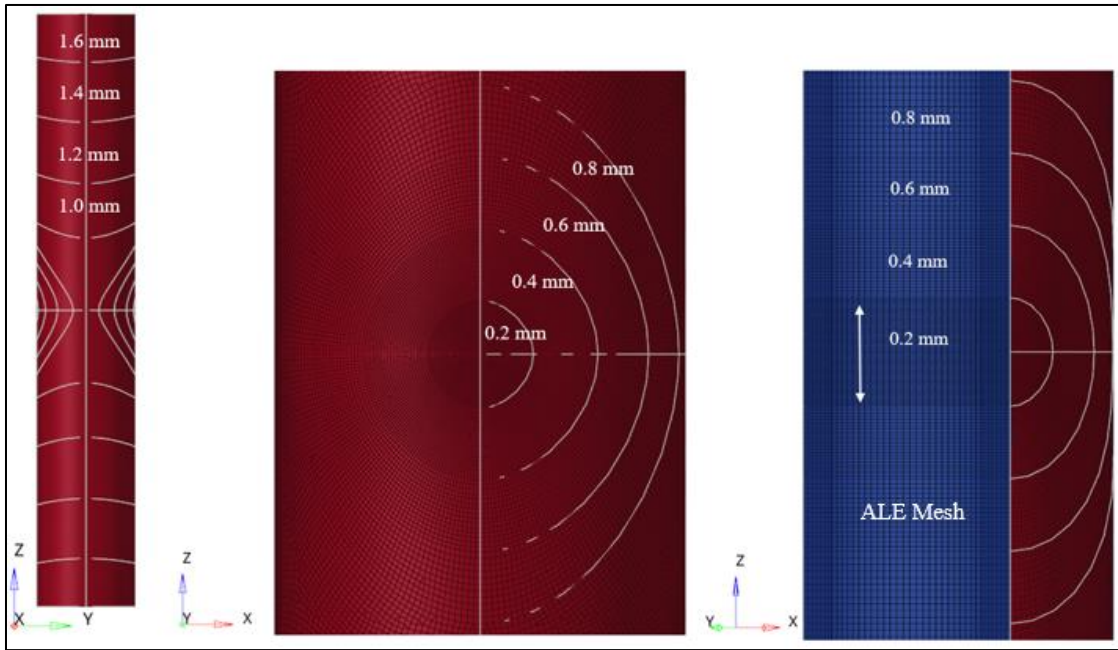


Figure 8. Mesh pattern and size

2.4 Equation of State

Equation of state (EOS) is a thermodynamic equation which defines the relationship between the variables such as pressure, volume, temperature, internal energies given that the matter does not undergo any chemical reaction or phase change. [6]

In this study, EOS (*EOS_LINEAR_POLYNOMIAL) is used to model the pressurized air and defines the relationship between pressure, volume and internal energy of air. *EOS_LINEAR_POLYNOMIAL is used to define coefficients of linear polynomial EOS, E0 and V0 to initialize thermodynamic state of material. See Appendix A.2.1 for the LS-Dyna EOS card image assigned to pressurized air.

Pressure is defined as following polynomial equation which is linear in terms of internal energy:

$$P = C_0 + C_1\mu + C_2\mu^2 + C_3\mu^3 + (C_4 + C_5\mu + C_6\mu^2)E$$

...Equation (1)

$$\text{with, } \mu = \frac{\rho}{\rho_0} - 1$$

Where,

P= Pressure, GPa

E= Internal energy per unit reference volume, GPa

C₀, C₁, C₂, C₃, C₄, C₅, and C₆ are the polynomial constants of equation of state.

ρ = current density, kg/mm³

ρ_0 = reference density defined in *MAT_NULL, kg/mm³

For simplification of our simulation, ideal gas modelling is considered. Ideal gas is modelled by setting C₀=C₁=C₂=C₃=C₆= 0 and C₄=C₅= $\gamma - 1$

γ is ratio of specific heat/adiabatic index = 1.4 for low temperature range gases.

Therefore, for ideal gas, pressure can be defined as,

$$p = (\gamma - 1) \frac{\rho}{\rho_0} E$$

Relative Volume, Vr is defined as ratio of current density to reference density. Initial relative volume V₀ can be given as ρ/ρ_0 at t =0 ms. For t=0, the density is equal to reference density. Therefore, V₀ can be set as 1 in EOS.

Internal energy per unit initial relative volume can be defined as:

$$E_0 = \frac{p_0}{\gamma - 1}$$

E₀ is the initial internal energy per unit reference volume, GPa

V₀ is initial relative volume.

p_0 is initial pressure, GPa

For example, for initial pressure of 50 psi (345e-6 GPa) E₀ can be given as,

$$E_0 = \frac{345 \times 10^{-6}}{(1.4 - 1)}$$

$$= 8.625e-4 \text{ GPa}$$

In current study, E_0 is calculated for three initial internal pressures of 50 psi (345e-6 GPa), 65 psi (448e-6 GPa) and 100 psi (690e-6 GPa).

2.5 Contact modelling

In the FE model, there are two types of interactions defined. First one being contact between pellet and glass tube (Structure to Structure). Similar contact as used by Sandesh Gandhi [4], *Contact_Automatic_Surface_To_Surface is used with SOFT=2 parameter. Second interaction defined in FE model is in between pressurized air and glass tube (Fluid to Structure) which is discussed in detail in further sections.

2.5.1 Pressurized Fluid Motion

*ALE_REFERENCE_SYSTEM_GROUP is assigned to pressurized air to define the motion of pressurized air throughout the simulation. This card is used to associate any part or mesh to reference system type. In simple words, it prescribes how certain mesh can translate, rotate, expand, contract or be fixed in space. See Appendix A.2.2 for the card image of *ALE_REFERENCE_SYSTEM_GROUP used in Finite Element model.

PRTYPE in card defines the reference system type. This model uses PRTYPE 4 which allows automatic mesh motion following mass weighted average velocity of ALE mesh. BCTRAN, BCEXP and BCROT defines translational, expansion and rotational constraints respectively. In current study, we only want the pressurized air to expand after crack propagation. Therefore, all X, Y and Z translational and rotational degrees of freedom are constrained for ALE mesh and is only allowed to expand. ICR defines the center point of expansion or contraction for ALE mesh. ICR =0 is set to make center of gravity of ALE mesh as an expansion or contraction center.

2.5.2 Coupling/ Interaction between Pressurized air and Glass tube

Figure 9 shows how coupling/ interaction between ALE and Lagrangian mesh takes place. Code searches for the penetration between Lagrangian mesh (glass tube) and ALE mesh (Pressurized air). Once it finds the penetration, it detects the NQUAD i.e. coupling points between ALE elements and Lagrangian elements. It tracks the independent motion of two materials over next time step dt and penetration distance is calculated. Then coupling force proportional to penetration distance is exerted on both the meshes. At each time step this cycle repeats which simulates fluid structure interaction.

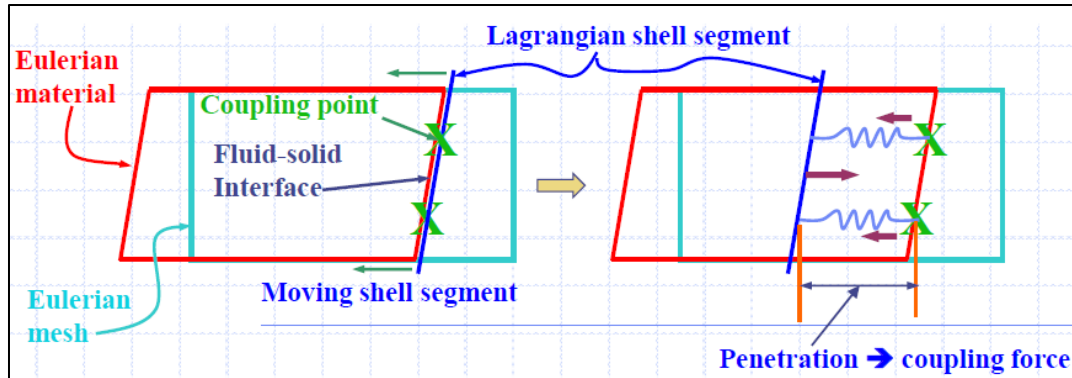


Figure 9. Standard penalty-based coupling

In order to define interaction between the pressurized air and the glass tube, coupling parameters must be defined. `*Constrained_Lagrange_In_Solid` is used to model this coupling between lagrangian mesh (glass tube) and ALE mesh (pressurized air). This card provides coupling mechanism to define fluid structure interaction. See Appendix A.2.3 for LS-Dyna card image of `*Constrained_Lagrange_In_Solid` used in FE model. Parameters used in `*Constrained_Lagrange_In_Solid` card are explained further.

SLAVE – Lagrangian mesh i.e. glass tube

MASTER – ALE mesh i.e. pressurized air

NQUAD – Number of coupling points distributed over each coupled Lagrangian surface segment. NQUAD depends on the relative mesh size of the interacting ALE and lagrangian elements. The change in coupling points after expansion must be taken in account and is recommended to have minimum NQUAD=2. If NQUAD is too few, then it can result in leaking while too many NQUAD can lead to instability. After calibrating the contact parameters, for current model NQUAD =4 gives most reliable results.

CTYPE – This parameter defines Fluid structure coupling method. As we have eroding shell elements present in FE model, EQ.4 which uses penalty coupling is selected.

DIREC – Defines the coupling direction. EQ. 1 us selected which considers normal direction for coupling under both compression and tension.

PFAC – Penalty factor. For hard structures and very compressible fluid like air, 0.1 PFAC is recommended by LS-Dyna solver.

FRIC – Coefficient of friction. It is kept as zero as frictionless contact allows maximum energy transfer.

NORM – This contact detects fluid only in one direction. This parameter defines which side of the shell segment will be considered for coupling with fluid. Therefore, it is important to align all shell normals in one direction. In given model, shell normals are

directed towards the ALE mesh. Therefore EQ. 0 is used which utilizes fluid on head side of Lagrangian segment normal for coupling. Figure 10 shows the how fluid and shell will interact for EQ. 0.

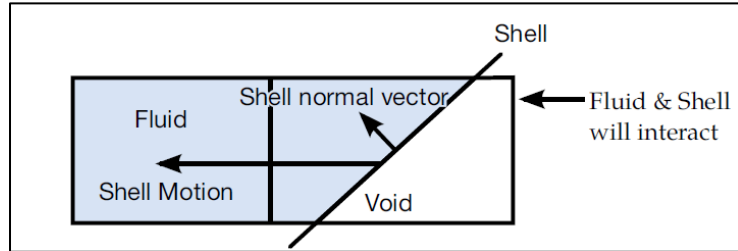


Figure 10. Required shell normal for fluid detection by code

IPENCHECK – Flag for initial penetration flag. This flag is turned off as Pressurized air mesh is model so that there is no initial penetration with glass tube.

INTFORCE – This flag enables or disables output of ALE coupling pressure and forces on slave Lagrangian surface. *DATABASE_BINARY_FSIFOR card is created when INTFORCE is selected as 1. This card defines the time interval between outputs.

All other parameters are taken as default.

*DATABASE_FSI keyword is defined to debug and fine tune the parameters mentioned above. This card controls the “dbfsi” which consists of coupling and leakage forces.

2.6 Failure strain calculation

Theoretical cohesive strength estimated from potential energy curve can be given by [7],

$$\sigma_c = \sqrt{\frac{E\gamma}{a_0}} \quad \dots Eq. (1)$$

Where,

E = Modulus of Elasticity, GPa

γ = Surface Energy, J/m²

a_0 = Equilibrium atomic separation, mm

In 1913, Inglis showed that applied stress σ_a is amplified at the ends of the major axis of the ellipse by studying plate containing elliptical hole, [7]

$$\sigma_{\max} = \sigma_a \left(1 + \frac{2a}{b} \right) \quad \dots \text{Eq. (2)}$$

where,

σ_{\max} = Maximum stress at the end of major axis, GPa

σ_a = Applied stress normal to major axis, GPa

a = Half major axis, mm

b = Half minor axis, mm

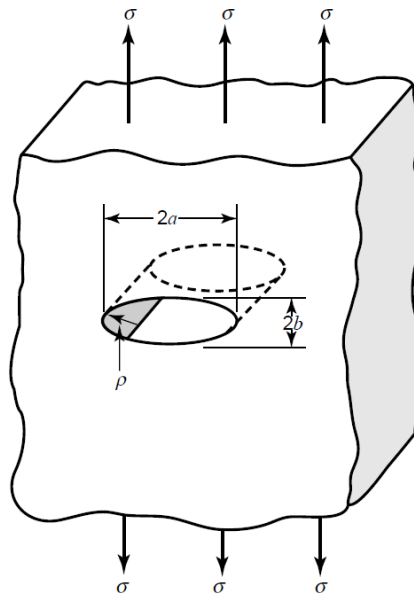


Figure 11. Stress applied to infinite plate with elliptical hole

Radius of curvature at end of the ellipse can be given as,

$$\rho = \frac{b^2}{a} \quad \dots \text{Eq. (3)}$$

From Eq.(2) and Eq.(3),

$$\sigma_{\max} = \sigma_a \left(1 + 2 \sqrt{\frac{a}{\rho}} \right)$$

For most cases, $a \gg \rho$, therefore,

$$\sigma_{\max} \approx 2\sigma_a \left(\sqrt{\frac{a}{\rho}} \right) \dots Eq. (4)$$

Also, $\rho \approx a_0$. With this approximation, Eq. (4) becomes,

$$\sigma_{\max} \approx 2\sigma_a \left(\sqrt{\frac{a}{a_0}} \right) \dots Eq. (5)$$

As shown in Figure 12. Assumption of elliptical flaw as crack., an elliptical flaw in a limit can be assumed as a crack.

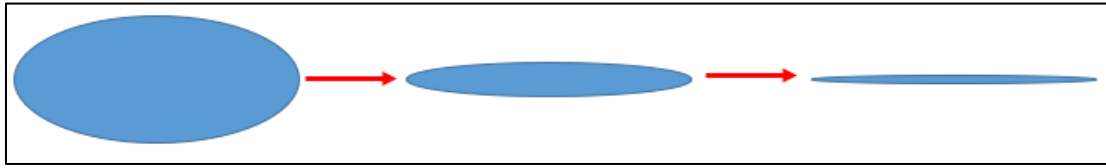


Figure 12. Assumption of elliptical flaw as crack

Fracture strength, $\sigma_f = \sigma_a[at\ failure]$

With above assumption, we can calculate the fracture strength by equating Eq. (1) and Eq. (5),

$$\begin{aligned} \sigma_c &= \sigma_{\max} \\ \sqrt{\frac{E\gamma}{a_0}} &= 2\sigma_f \sqrt{\frac{a}{a_0}} \\ \sigma_f &= 0.5 \sqrt{\frac{E\gamma}{a}} \dots Eq. (6) \end{aligned}$$

Where, a = half width flaw size in mm.

3-point bending experiments were carried out on grounded borosilicate glass bars to estimate flaw size and fracture energy by Mecholsky J. J., Rice R. W. and Freiman S. W. [8]. Following values of flaw size and fracture energy measured in the article [8] is used to calculate the fracture strength in current study: $a = 0.08$ mm and $\gamma = 4$ J/m²

After substituting the values of flaw size, fracture energy and elastic modulus, we get fracture strength,

$$\sigma_f = 0.028 \text{ GPa}$$

As Stress- Strain diagram for glass is linear, we can calculate strain at failure from Hooke's law,

$$\varepsilon_f = \frac{\sigma_f}{E} = 0.000445$$

3 Challenges and Limitations

3.1 *Constrained_Lagrange_in_Solid contact parameter calibration

Constrained Lagrange in Solid (CLiS) contact uses either standard penalty-based algorithm or segment-based penalty method. In standard penalty-based contact, ALE nodes are coupled to Lagrange segments while in segment-based contact ALE segments are coupled to Lagrange segments. As discussed in previous section, standard penalty-based algorithm is used for fluid structure interaction. Depending on the penetration distance and location of penetration, springs are created at coupling points. Parameters defined in CLiS card decides the spring stiffness and in turn the spring force applied between fluid and structure. If coupling spring stiffness is low then there will be leakage and if the spring is too stiff, there can be instability in simulation. Few trial simulations were carried out to understand the effect of each parameter on the Fluid-Structure Interaction with coarse mesh. Average pressure and leakage forces were studied for these simulations to understand if there is any leakage or stiff contact.

3.2 Meshing

In the finite model, both crack propagation and fluid-structure interaction are sensitive to mesh size and pattern. For results closer to experimental data, the first model was built as per the recommendations of previous students [4,5]. Following modifications were done to accommodate the ALE technique:

1. ALE algorithm is highly expensive as compared to Lagrangian method due to additional computational cost for advection, coupling force calculation and interface reconstruction. Additional solid elements used for ALE modelling contributes to this cost too. To reduce computational time, minimum mesh size was changed from 0.1 mm to 0.2 mm and varying mesh with factor of 2 is used for glass tube.
2. Ratio of Lagrange segment and ALE segment affects the number of coupling points between fluid and structure. ALE part is meshed with similar gradient as glass tube to keep this ratio closer to 1:1. Although, for 1:1 ratio NQUAD=2 is recommended, for current FE model leakage was noticed. This might be due to the difference in mesh pattern of glass tube and pressurized air ALE mesh. From trial simulations, it was found that NQUAD (Number of coupling points) =4 gives expected results.
3. It is recommended to use ELFORM=11 in *SOLID_SECTION for ALE mesh. Therefore, simulations were carried out with Hexahedral and Tetrahedral Elements. Although, Tetrahedral elements allows meshing of complex parts, it led to numerical instability during simulation. Hence, Hexahedral elements were selected for ALE mesh for final FE model.

4. For fluid-structure interaction between pressurized air and glass tube it was necessary to model an enclosed volume for ALE mesh. To accommodate this requirement, an enclosing fixed plate was modelled at the bottom of the tube instead of using Single point constraints at lower surface of glass tube.

3.3 Size of output files

Due to combination of element erosion and ALE method in FE model, output files created for each simulation are in order of 60-80 GBs. As we need number of simulations to study the effect of strain values and internal pressure, it becomes difficult to store and manage so many huge output files. As we are specifically interested in the results near the crack event, output file frequency is increased from 0.5 ms to 0.8 ms and decreased for remaining part of the simulation. This way we have dense data only for the time period of focus. For this purpose, LCDT curve is defined in *DATABASE_BINARY to control the time interval between d3plot file creation. Figure 13. Load curve defining d3plot output interval shows used load curve.

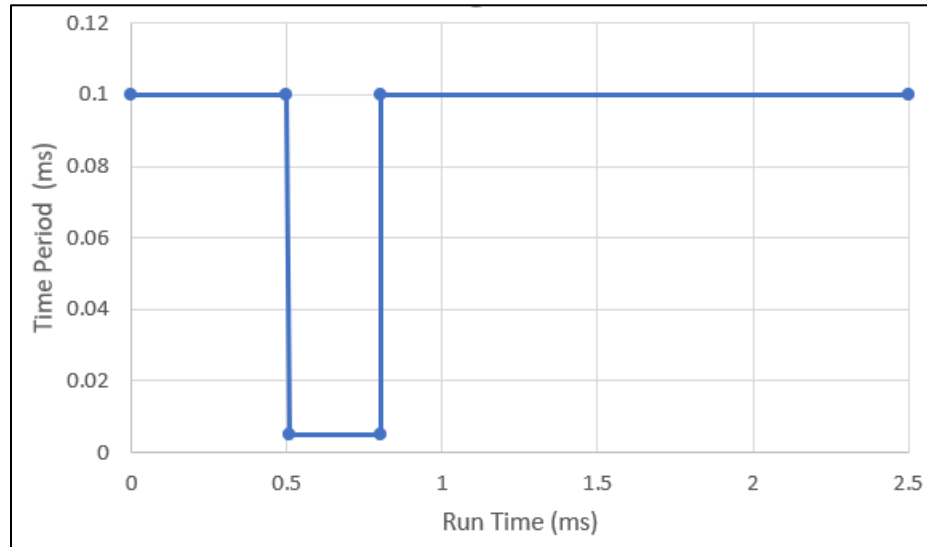


Figure 13. Load curve defining d3plot output interval

3.4 Internal Pressures

ALE compressible flow solver algorithm in LS-DYNA has been developed with the intent of short duration problems with high pressure and velocity gradients. The solver is not suitable for low pressure gradients or long duration simulations. Initially, simulations were carried out for 10, 50, 65 and 100 psi internal pressures to have results over wider pressure variations. For 10 psi internal pressure, simulation ran into numerical instability and was unable to completely solve the analysis. Therefore, only 50, 65 and 100 psi internal pressures are considered for this project.

4 Results and Correlation

In this study, the implementation of ALE is verified by comparing crack pattern and broken glass size with experiments. Results for recommended failure strain and calculated strain along with different internal pressures are discussed.

4.1 Comparison of Results for $3.5e-5$ and $4.45e-4$ Failure Strain

In previous study carried out by Sandesh Gandhi, failure strain of $3.5e-5$ was calibrated by correlating crack pattern found in experiments and simulation. As recommended, initially $3.5e-5$ failure strain value is used to carry out simulation with internal pressure of 50 psi. But as shown in Figure 14, glass shatters completely within 0.1 ms. More than 90% of glass elements have been eroded at 0.1 ms itself. Figure 14 shows, remaining shattered elements. This is even before the 50 psi internal pressure is reached. This behavior wasn't present when Vijay Thanati carried out simulation to study effect of internal pressure. This difference can be because the method of pressure application used before. Before, the pressure drop after crack propagation was estimated. In current study, we have modelled pressurized fluid itself to simulate fluid-structure interaction.

Based on the simulation results seen in Figure 14, it was observed that higher failure strain is needed to get closer to experimental results. Therefore, new failure strain is calculated explained in section 2.6. Results found with new calculated failure strain i.e. $4.45e-4$ have better correlation with experiments explained later in report.

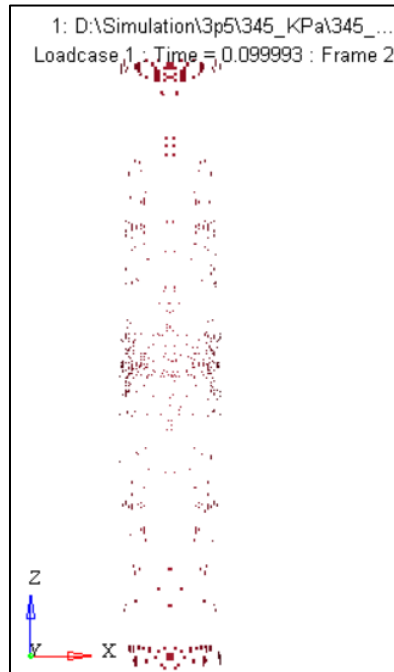


Figure 14. Glass tube shattering at $t = 0.01$ ms for $3.5e-5$ failure strain

4.2 Verification of Results

It is important to check if the calculated results are correct and can be relied upon. This can be verified by ensuring that the specified internal pressure is achieved and observing the pressure drop curve throughout the simulation. The fluid-structure interaction is checked using *DATABASE_FSI card which creates a dbfsi output file containing average pressure on Lagrangian surface and leakage forces. This file is used to verify if the input pressure is applied while simulation and if coupling between pressurized air and glass tube working accurately.

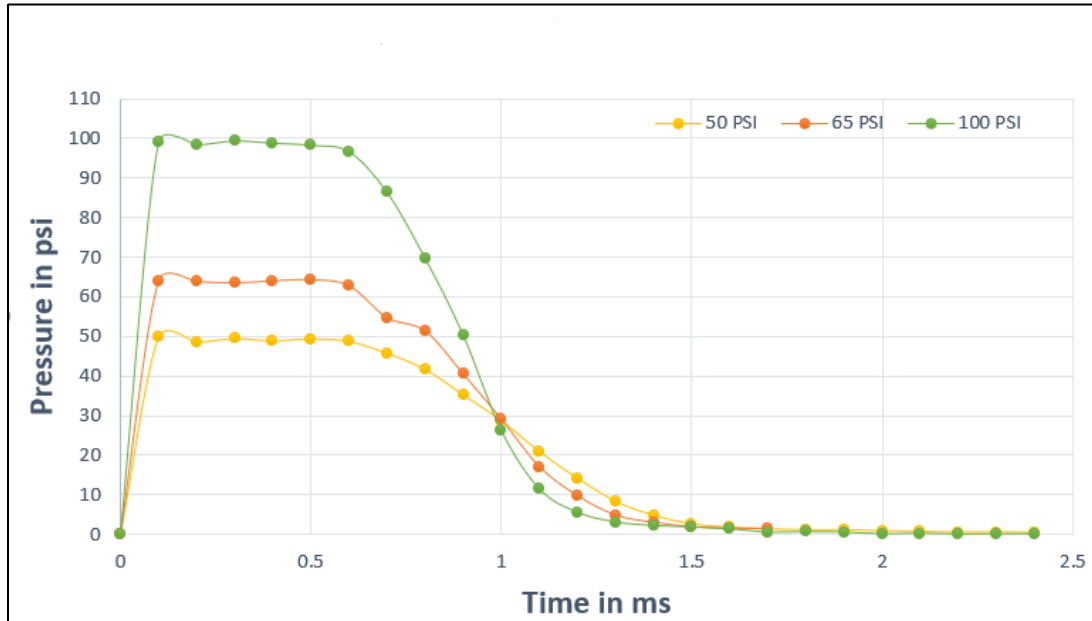


Figure 15. Average pressure Vs time output from dbfsi file

Figure 15 shows average pressure applied on Lagrangian surface for 50 psi, 65 psi and 100 psi internal pressures obtained from dbfsi file. It is observed that the average pressure experienced by Lagrangian surface is approximately equal to input internal pressure. Pellet initial velocity is activated at 0.5 ms and pellet impacts the glass tube for the first time within few microseconds. The pressure curve seen verifies this scenario, where pressure drops right after 0.5 ms as pressurized fluid continues to flow out of tube. This is the expected behavior and therefore we can say the fluid-structure interaction is working. X, Y, Z leakage forces are checked for the simulations. It is made sure that the leakage forces are zero.

4.3 Correlation with Experimental Data

Two parameters are selected to compare the simulations with experimental results, Crack pattern and broken glass size. Figure 16 shows the stills of pellet impact experiment. From stills it is apparent that the glass size at either ends of glass tube reduces as internal pressure goes up. A similar trend is observed in simulations as shown in Figures 17.

After careful visual inspection, the crack pattern observed in simulations for 50, 65 and 100 psi internal pressures match reasonably good with stills captured with high speed camera in experiments.

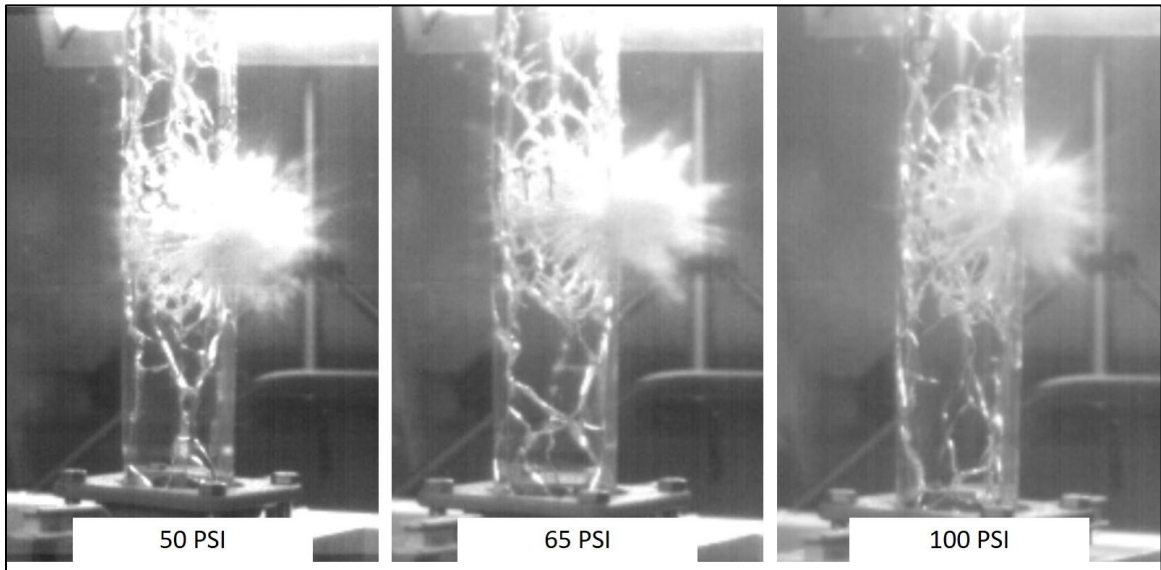


Figure 166. Stills from pellet impact experiment for 50, 65 and 100 psi internal pressure

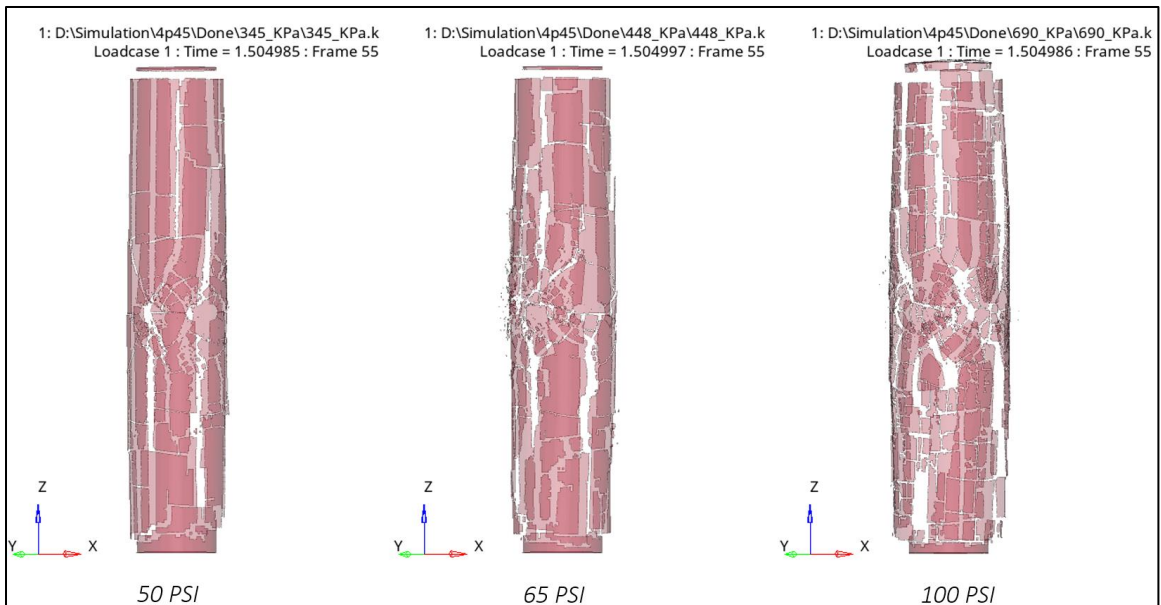


Figure 17. Crack pattern after pellet impact for 50, 65 and 100 psi internal pressure

After experiments, USBR collected the 10 largest broken glass samples. Maximum and average broken glass size was estimated from these samples. Similarly, surface area of largest 5 glass pieces was measured in Hypermesh. Table 7 compares the experimental and simulation results found. As seen in Table 7, average and maximum surface area of broken glass pieces calculated in simulation are fairly close to estimated value in experiments.

Table 7. Comparison of broken glass size between simulation and experiment

Pressure (PSI)	Surface Area of Largest 5 Glass Pieces in FEA (cm ²)	Simulation (cm ²)		Experiment (cm ²)	
		Average	Maximum	Average	Maximum
50	26.46	18.6	26.46	14.01	24.73
	21.02				
	16.45				
	14.55				
	14.52				
65	18.8	17.256	18.8	9.167	18.28
	18.61				
	17.86				
	15.64				
	15.37				
100	14.3	11.762	14.3	7.75	15.96
	13.17				
	11.25				
	11.25				
	8.84				

5 Conclusion

A FE model is developed using the ALE method for simulating pellet impact on a pressurized glass tube in LS-DYNA and validated using experimental test data. This study showed that the ALE technique in LS-DYNA provides reasonable results for fluid-structure interaction. It is observed that the current simulation captures crack propagation and pressure drop after impact reasonably well. Comparison with experimental data is done with respect to crack pattern, average and maximum glass size. Fairly good comparison is found between simulation and experimental results.

The effect of various internal pressure and failure strain values was studied. It was observed that for calculated failure strain value i.e. 4.45×10^{-5} , results correlate reasonably. Results for 50, 65 and 100 psi are considered for comparison. It is apparent that the glass size reduces significantly with increased internal pressure.

FE modelling technique is explained in detail along with numerical and theoretical background. The FE model can be utilized to study different material models to devise a countermeasure for bushing failures. In future studies, Geometric/material modifications can be done in existing model or simpler FE model with pressure results mapped to nodes/elements.

6 Recommendations

This study focuses towards the implementation of ALE to improve correlation between simulation and experimental results. There is still scope of improvements which can improve the results achieved through simulation.

- Although, we have developed the technique for fluid-structure interaction for our problem statement, the computational cost associated with this implementation is high too as compared to previous FE models. For further study, the pressure drop curve calculated for 50, 65 and 100 psi internal pressure can be mapped as a boundary condition. This will reduce the computational time while keeping the accuracy of result reasonably good in terms of crack pattern and glass size.
- In current model, ideal gas is assumed for simplification of problem. Taking this model further, it is recommended to use the material properties like viscosity and density of fluid used in bushings while developing the countermeasure.
- Current crack propagation method is highly dependent on mesh size and pattern. Other techniques with relatively less dependency on mesh can be explored to simulate the crack.

7 Reference List

- [1] Gilani, Amir & Whittaker, Andrew & Fenves, Greg. (1999). Seismic evaluation of 550 kV porcelain transformer bushings. 10.13140/RG.2.1.4994.2649.
- [2] Beck, Kevin. "What Is the Purpose of a Transformer?" sciencing.com, <https://sciencing.com/purpose-transformer-4620824.html>. 19 October 2019.
- [3] 'Sniper Attack On Calif. Power Station Raises Terrorism Fears', the two-way, www.npr.org
- [4] Sandesh Suresh Gandhi, 'Simulation of Crack Pattern on Borosilicate Glass Cylinder Under Pellet Impact'
- [5] Vijay Thanati, 'Simulation of Crack Pattern on Borosilicate Glass Cylinder Under Pellet Impact'
- [6] Livermore Software Technology Corporation (LSTC), "LS-DYNA Keyword User's Manual, Volume 2"
- [7] Hertzberg, Richard W., Vinci, Richard P., Hertzberg, Jason L.. Deformation and Fracture Mechanics of Engineering Materials. United States: Wiley, 2012.
- [8] Mecholsky J. J., Rice R. W. and Freiman S. W. (1974), Prediction of Fracture Energy and Flaw Size in Glasses from Measurements of Mirror Size. Journal of the American Ceramic Society, 57: 440-443.

A Appendix

A.1 Properties of Borosilicate Glass

Product
Information

SCHOTT

BOROFLOAT® Borosilicate Float Glass

Schott offers a highly chemically resistant borosilicate glass with a low thermal expansion that is being manufactured by the float method. BOROFLOAT® is a technologically significant development, achieving unsurpassed quality for flat borosilicate glass. It replaces TEMPAX®, a drawn flat borosilicate glass. The high quality resulting from the float glass process opens up new applications for borosilicate flat glass, which has proven itself over time in laboratories, chemical process plants and in the home appliance and lighting industries.

BOROFLOAT® flat glass is highly resistant to water, neutral, acidic and saline solutions; as well as to chlorine, bromine, iodine and organic substances. Even over long periods of time and at high temperatures that exceed 100°C, BOROFLOAT® exceeds the chemical resistance of most metals and other materials.

Chemical Data

- Hydrolytic Resistance (ISO-719-HGB) 1
- Hydrolytic Resistance (ISO 720-HGA) 1
- Acid Resistance (ISO 1776) 1
- Alkali Resistance (ISO 695-A) 2

Mechanical Properties

- Density (@ 25°C/77°F) 2.23 g/cm³
- Modulus of Elasticity 63 kN/mm²
- Knoop Hardness HK 0.1/20 480
(according to E DIN/ISO 9385)
- Poisson's Ratio 0.2

Electrical Properties

- Dielectric Constant (@ 1 MHz & 25°C) 4.6
- Loss Tangent (@ 1 MHz & 25°C) 37 x 10⁻⁴
- Dielectric Strength(@ 50 Hz & 25°C) 16 kV/mm
- Electric Volume Resistivity (log ρ)
 - @ 250°C 8.0
 - @ 350°C 6.5

Physical Impact

The resistance of BOROFLOAT® to physical impact depends on the type of installation, the size and thickness of the glass panel, the type of physical impact, in addition to other parameters.

Optical Properties

- Refractive Index (n_d) 1.472
- Dispersion (n_F - n_C) 71.9 x 10⁻⁴

Thermal Properties

- Linear Thermal Coefficient of Expansion α (20-300°C/ 68-572°F) 3.25 x 10⁻⁶/K
- Transformation Temperature T_g 530°C/986°F
- Annealing Point (10¹³ dPa-s) 560°C/1040°F
- Softening Point (10^{7.5} dPa-s) 815°C/1508°F
- Thermal Conductivity k
 - @ 90°C 1.12 W/(m·K)
 - @ 194°F 0.65 Btu·ft/h·ft²·°F
- Mean Specific Thermal Capacity c_p
 - 20-100°C 0.83 kJ/(kg·K)
 - 68-212°F 0.19 Btu/lb·°F
- Maximum Operating Temperature (Considering RTD¹)
 - Short term 500°C/932°F
 - Long term 450°C/842°F
- Resistance to Temperature Differences (RTD¹)
 - Short term exposure
 - (1 hour) 110K/198°R
 - (1-100 hours) 90K/162°R
 - Long term exposure (>100 hours) 80K/144°R
- Resistance to Thermal Shock (RTS²)
 - Thickness <4 mm 175K/315°R
 - Thickness 4-6 mm 160K/288°R
 - Thickness 6-15 mm 150K/270°R
 - Thickness >15 mm 140K/252°R

SCHOTT North America, Inc.

5530 Shepherdsville Rd.
Louisville, KY 40228

Phone: (502) 657-4417

Telefax: (502) 966-4976


Email: info@us.schott.com

www.us.schott.com

1204
Supersedes All Previous Releases


A.2 LS-Dyna Card Images

A.2.1 Equation of state card image

 Keyword Input Form


NewID	RefBy	Add	Accept	Delete	Default	Done		
<input type="checkbox"/> Use *PARAMETER						(Subsys: 1)	Setting	
*EOS_LINEAR_POLYNOMIAL_(TITLE) (1)								
TITLE								
EOS_Inside_pressure								
1	<u>EOSID</u>	<u>C0</u>	<u>C1</u>	<u>C2</u>	<u>C3</u>	<u>C4</u>	<u>C5</u>	<u>C6</u>
	4	0.0	0.0	0.0	0.0	0.4000000	0.4000000	0.0
2	<u>E0</u>	<u>V0</u>						
	8.625e-04	1.0000000						

A.2.2 ALE Reference System Group card image

 Keyword Input Form

NewID	Pick	Add	Accept	Delete	Default	Done		
<input type="checkbox"/> Use *PARAMETER						(Subsys: 1)	Setting	
*ALE_REFERENCE_SYSTEM_GROUP (1)								
1	<u>SID</u>	<u>STYPE</u>	<u>PRTYPE</u>	<u>PRID</u>	<u>BCTRAN</u>	<u>BCEXP</u>	<u>BCROT</u>	<u>ICOORD</u>
	3	1	4	0	7	0	7	0
2	<u>XC</u>	<u>YC</u>	<u>ZC</u>	<u>EXPLIM</u>	<u>EFAC</u>	<u>UNUSED</u>	<u>FRCPAD</u>	<u>IEXPND</u>
	0.0	0.0	0.0	0.0	0.0	0	0.0	0
3	<u>IPDXCL</u>	<u>IPIDTYP</u>						
		0						

A.2.3 Constrained Lagrange in Solid Contact card image

 Keyword Input Form

NewID	Pick	Add	Accept	Delete	Default	Done		
<input type="checkbox"/> Use *PARAMETER						(Subsys: 1)	Setting	
*CONSTRAINED_LAGRANGE_IN_SOLID (1)								
1	<u>COUPID</u>	<u>TITLE</u>						
	3	AIR_GLASSTUBE_INTERACTION						
2	<u>SLAVE</u>	<u>MASTER</u>	<u>SSTYP</u>	<u>MSTYP</u>	<u>NQUAD</u>	<u>CTYPE</u>	<u>DIREC</u>	<u>MCOUP</u>
	2	1	0	0	4	4	1	1
3	<u>START</u>	<u>END</u>	<u>PFAC</u>	<u>ERIC</u>	<u>FRCMIN</u>	<u>NORM</u>	<u>NORMTYP</u>	<u>DAMP</u>
	0.0	1.000e+01	0.100000	0.0	0.2000000	0	0	0.0
4	<u>CQ</u>	<u>HMIN</u>	<u>HMAX</u>	<u>ILEAK</u>	<u>PLEAK</u>	<u>LCIDPOR</u>	<u>NVENT</u>	<u>BLOCKAGE</u>
	0.0	0.0	0.0	1	0.0100000	0	0	0
5	<u>IBOXID</u>	<u>IPENCHK</u>	<u>INTFORC</u>	<u>IALESOF</u>	<u>LAGMUL</u>	<u>PFACMM</u>	<u>THKF</u>	
	0	0	1	0	0.0	0	0.0	